HHS Public Access

Author manuscript

ChemMedChem. Author manuscript; available in PMC 2018 April 12.

Published in final edited form as:

ChemMedChem. 2017 December 07; 12(23): 1942–1952. doi:10.1002/cmdc.201700614.

Design, Synthesis, Biological Evaluation, and X-ray Studies of HIV-1 Protease Inhibitors with Modified P2′ Ligands of Darunavir

Prof. Dr. Arun K. Ghosh[a], **Dr. W. Sean Fyvie**[a], **Margherita Brindisi**[a], **Dr. Melinda Steffey**[a], **Dr. Johnson Agniswamy**[b], **Dr. Yuan-Fang Wang**[b], **Dr. Manabu Aoki**[c], **Dr. Masayuki Amano**[c], **Prof. Dr. Irene T. Weber**[b], and **Dr. Hiroaki Mitsuya**[c,d,e]

[a]Department of Chemistry and Department of Medicinal Chemistry, Purdue University, West Lafayette, IN 47907 (USA)

[b]Departments of Biology and Chemistry, Molecular Basis of Disease, Georgia State University, Atlanta, GA 30303 (USA)

[c]Departments of Hematology and Infectious Diseases, Kumamoto University School of Medicine, Kumamoto 860-8556 (Japan)

[d]Experimental Retrovirology Section, HIV and AIDS Malignancy Branch, National Cancer Institute, Bethesda, MD 20892 (USA)

[e]Center for Clinical Sciences, National Center for Global Heath and Medicine, Shinjuku, Tokyo 162-8655 (Japan)

Abstract

The structure-based design, synthesis, and biological evaluation of a series of nonpeptidic HIV-1 protease inhibitors with rationally designed P2′ ligands are described. The inhibitors are designed to enhance backbone binding interactions, particularly at the S2′ subsite. Synthesis of inhibitors was carried out efficiently. The stereochemistry of alcohol functionalities of the P2′ ligands was set by asymmetric reduction of the corresponding ketone using (*R*,*R*)- or (*S*,*S*)-Noyori catalysts. A number of inhibitors displayed very potent enzyme inhibitory and antiviral activity. Inhibitors **3g** and **3h** showed enzyme K_i values of 27.9 and 49.7 pM and antiviral activity of 6.2 and 3.9 nM, respectively. These inhibitors also remained quite potent against darunavir-resistant HIV-1 variants. An X-ray structure of inhibitor **3g** in complex with HIV-1 protease revealed key interactions in the S2′ subsite.

Keywords

drug resistance; HIV-1 protease inhibitors; P2′ ligands; pharmacokinetics; structure-based design

Correspondence to: Arun K. Ghosh.

Supporting information and the ORCID identification number(s) for the author(s) of this article can be found under: https://doi.org/10.1002/cmdc.201700614.

Conflict of interest

The authors declare no conflict of interest.

Introduction

The arrival of HIV/AIDS in the early 1980s marked the onset of a global pandemic.[1,2] This led to intense worldwide research efforts in academic and pharmaceutical laboratories for treatment of HIV infection and AIDS.[3,4] Enormous research advances in the mid-1990s fundamentally changed the prognosis of HIV/AIDS treatment and management of the disease. The advent of combined antiretroviral therapy (cART), involving the use of HIV-1 protease inhibitors (PIs) and reverse transcriptase inhibitors drastically improved life expectancy and decreased HIV-related mortality of patients with access to this treatment regimen.[5,6] Recent improvement of first line cART and declines in the price of treatment have prompted further accessibility of cART to developing countries.[7,8] Despite these great strides, there are serious limitations to current treatment regimens including cost, toxicity, patient compliance, side effects, and resistance. Perhaps, the most imposing limitation is the rapid rate at which the HIV generates viable drug-resistant mutants under selection pressure.[9,10] PIs are an integral part of some of the most preferred cART treatment regimens.[11,12] In our continuing efforts to develop PIs to combat drug resistance, we designed several classes of novel compounds that display exceptional antiviral potencies across wild-type and multidrug-resistant HIV strains.[13,14] Inhibitor **1** (TMC-114 or darunavir, DRV, Figure 1) displayed picomolar enzyme inhibitory activity and potent antiviral activity.[15,16] It was also endowed with unprecedented activity against a range of known multidrug resistant HIV strains.[17,18] Darunavir received FDA approval in 2006 for use in adult patients harboring drug-resistant strains.[15,16] In 2008, it was approved for all HIV/AIDS patients and emerged as a front line anti-HIV therapy for use in both adult and pediatric patients.[19]

Our X-ray structural analysis of DRV-bound HIV-1 protease structure revealed an extensive network of hydrogen bonding interactions between DRV and backbone atoms of HIV-1 protease.[20] In particular, the *bis*-THF P2 ligand formed a pair of strong hydrogen bonds with Asp29 and Asp30 NHs in the S2 subsite. The P2′-aminosulfonamide forms a pair of hydrogen bonds with Asp30′ backbone amide NH as well as with the Asp30′ backbone carbonyl oxygen. These backbone interactions have been attributed to DRV′s wide range of activity against known PI-resistant mutants.[15,21] The *bis*-THF ligand is a privileged ligand for DRV and its extensive interactions are responsible for DRV′s unique activity. Over the years, we have investigated other structurally intriguing ligands that mimic the ligand-binding interactions of the *bis*-THF ligand of DRV in the S2 subsite. In an effort to promote further ligand-binding site interactions in the S2′ subsite, we have explored modifications of the P2′ ligand with hydrogen-bonding donor/acceptor groups to form enhanced backbone interactions. We are particularly interested in ligands and scaffolds that may improve metabolic stability. In a preliminary effort, based on the X-ray structure of DRV and HIV-1 complex, we incorporated carboxylic acid and carboxamide functionalities at the 4-position of the benzene ring of the P2′-sulfonamide ligand.[22,23] Both the carboxylic acid and the carboxamide ligand showed very potent picomolar enzyme inhibitory activity. The carboxamide ligand derived inhibitor **3b** showed potent antiviral activity. To obtain ligand-binding site interactions of the carboxamide derivative, we determined an X-ray structure of **3b**-bound HIV-1 protease.[23] The key inhibitor-binding site interactions are shown in Figure 2A. In particular, the P2′ moiety of **3b**, similarly to DRV, shows hydrogen-bond interactions

with the backbone of Asp30′. Interestingly, the P2′ benzamide moiety of **3b** also showed a conserved water-mediated bridging hydrogen bond with Gly48′ (Figure 2B).[24] Based on this structure, we have now further modified the P2′ ligand to promote hydrogen bonding interactions and improve antiviral activity using a range of stereochemically defined functionalities and heterocyclic scaffolds. Herein we report the structure-based design, synthesis, X-ray structural studies and biological investigation of a series of HIV-1 PIs with novel P2′ ligands.

Results and Discussion

Synthesis of ligands and inhibitors

All target PIs herein presented are accessible via diacetate intermediate **5**, which has been prepared in two steps from commercially available chiral epoxide **4** as described previously.[25] The synthesis of compounds **3a**–**f** is reported in Scheme 1. Deprotection of **5** to the corresponding aldehyde with potassium carbonate in methanol and subsequent Pinnick oxidation led to the key carboxylic acid intermediate **7** in excellent yield. Compound **7** was treated with trifluoroacetic acid (TFA) to remove the Boc group and the resulting TFA salt was treated with the known *bis*-THF activated carbonate **6**[26] in a 10:1 mixture of acetonitrile/water in the presence of *N,N*-DIPEA to provide inhibitor **3a**. Carboxamide inhibitor **3b** was prepared via direct one-pot conversion of inhibitor **3a** to a mixed anhydride with di-*tert*-butyldicarbonate in the presence of pyridine followed by condensation with ammonium carbonate in 76% yield.[27]

Treatment of acid **7** with isobutyl chloroformate in the presence of *N*-methylmorpholine, followed by *N,O*-dimethylhydrox-ylamine led to the corresponding Weinreb amide **8**. Exposure to TFA followed by treatment with activated carbonate **6** and *N,N*-DIPEA in acetonitrile led to inhibitor **3c**. Intermediate **8** was also converted into its methyl ketone derivative by exposure to methylmagnesium bromide in dry THF. Boc deprotection followed by reaction with *bis*-THF derivative **6** led to final compound **3d**.

Inhibitors **3e**,**f** were prepared starting from compound **3d**. Exposure of **3d** to a catalytic amount (0.5 mol%) of the (*R,R*)-or (*S,S*)-Noyori catalysts[28] in a 1:2 ratio of Et_3N/HCO_2H led to high yields (95–98%) of the corresponding (*R*) and (*S*) final alcohols **3e** and **3f**, respectively, with excellent enantioselectivity (see Experimental Section for details).

The synthesis of oxazole-containing inhibitors **3g**,**h** is reported in Scheme 2. Key carboxylic acid intermediate **7** was submitted to coupling reaction with serine methyl ester hydrochloride in the presence of EDCI, HOBt and *N,N*-DIPEA in dry DMF affording the corresponding amide adduct in 91% yield.

Subsequent dehydrative cyclization conditions with DAST reagent at −78°C afforded the corresponding oxazoline intermediate immediately submitted to a radical bromination-reductive elimination protocol using $DBU/BrCCl_3$ providing oxa-zole derivative **9** in 64% yield over two steps.[29] The reduction of the ester functionality of oxazole **9** with $NaBH_4$ in absolute ethanol provided the corresponding hydroxymethyl intermediate in moderate yield.

Both the oxazole ester **9** and its hydrox-ymethyl derivative were converted into the corresponding final inhibitors **3g**,**h** via standard methods.

The second series of oxazole inhibitors **3i**–**l** was prepared as shown in Scheme 3. Diacetate intermediate **5** was converted into the oxazole derivative **10** in high yield employing the procedure reported by van Leusen and co-workers with toluene-sulfonylmethyl isocyanide (TosMIC) in the presence of K_2CO_3 in methanol.[30] Exposure of compound **10** to TFA followed by treatment with activated *bis*-THF derivative **6** in the presence of *N,N*-DIPEA led to inhibitor **3i**. Intermediate **10** was also treated with isopropylmagnesium chloride providing the 2-mag-nesiate derivative which was immediately reacted with the acetate-derived Weinreb amide to give the desired 2-acetyl ox- azole **11** in good yield.[31] Acetyl derivative **11** underwent Boc-deprotection with TFA and treatment with activated *bis*-THF derivative **6** in the presence of *N,N*-DIPEA providing inhibitor **3j**. This latter also underwent Noyori asymmetric hydrogenation with both the (*R,R*)- or (*S,S*)-Noyori catalysts in a 1:2 ratio of Et_3N/HCO_2H leading to final compounds **3k**,**l** in high yields and enantiomeric excess (see Experimental Section for details).

Biological assays

We evaluated all synthetic inhibitors in a HIV-1 protease inhibitory assay using the protocol developed by Toth and Mar-shall.[32] These results are shown in Table 1. Selected potent inhibitors were further evaluated in an antiviral assay following a reported protocol using MT-2 cells exposed to HIV-1_{LAI}.[33] In an attempt to promote hydrogen bond formation with the back bone atoms at S2′ subsite, we investigated the feasibility of carboxylic acid, and various derivatives. As shown, incorporation of a *para*-carboxylic acid functionality provided inhibitor **3a** which showed very potent HIV-1 inhibitory activity (K_i=12 pM). However, this carboxylic acid derivative showed an antiviral IC_{50} value greater than 1 μM. Interestingly, the corresponding carboxamide derivative **3b** not only showed very potent HIV-1 protease inhibitory activity, but also displayed potent antiviral activity (IC_{50}=45 nM). The reason for the poor antiviral activity for compound **3a** may be due to the low cell penetration ability of carboxylic acids. Based on the X-ray structure of DRV-bound HIV-1 protease, we speculated that the carbonyl group of a carboxylic acid derivative or the heteroa-toms of the corresponding heterocyclic derivatives can interact with backbone atoms, particularly Asp29′ and Asp30′ backbone NHs. We therefore investigated other carbonyl derivatives such as the methoxymethyl amide in inhibitor **3c** as well as the methyl ketone derivative in inhibitor **3d** (entries 3, 4). Interestingly, methyl ketone derivative **3d** displayed very potent enzyme K_i as well as antiviral activity. We have examined inhibitory properties of the corresponding reduced products, **3e** and **3f** (entries 5, 6). The stereochemical effect is apparent, as compound **3e** with (*R*)-hydroxy configuration has shown a greater than fourfold improvement in enzyme K_i. Compound **3e** has also shown potent antiviral IC_{50} of 4 nM.

We then pursued carboxylic acid bioisosteres with a series of oxazole-derived P2′ ligands. As shown, compound **3g** and **3h**, bearing, respectively, a methyl ester and a hydroxymethyl functionality at the 4-position of the 2-phenyloxazole moiety, displayed a slight decrease of enzyme inhibitory potency with K_i=27.9 and K_i=49.7 pM, respectively (entries 7 and 8). The corresponding reduced product alcohol **3h** displayed a slightly improved antiviral IC_{50}

value of 3.9 nM. We have also synthe-sized a series of carboxylic acid derivatives with 5-phenyloxa-zole scaffolds (entries 9–12). These derivatives displayed decreased enzyme inhibitory potency; however, they maintained excellent antiviral activity similar to that of DRV. Monosubsti-tuted derivative **3i** showed a K_i of 126 pM and an antiviral IC_{50} value of 2.8 nM (entry 9). Incorporation of methyl ketone at the 2-position of the oxazole ring provided **3j**. This substitution did not improve potency and showed activity similar to **3i** (entry 10). Reduction of the methyl ketone provided stereo-chemically defined alcohols with (*R*)- and (*S*)-configuration. Both derivatives showed potent antiviral activity, however, no improvement was observed over monosubstituted oxazole derivative **3i** (entries **11** and **12**).

Because compound **3g** contains an interesting heterocyclic P2′ ligand, we planned to obtain molecular insight into its binding properties using an X-ray structure. To this end, we determined the X-ray structure of **3g**-bound HIV-1 protease. To further correlate the structure with its antiviral properties, we examined both potent oxazole containing PIs (**3g**, **3h**) against DRV-resistant HIV-1 variants. In these assays, MT-4 cells were exposed to wild-type HIV-1 and three drug-resistant variants HIV-$1_{DRV}{}^{R}{}_{20}$, HIV-$1_{DRV}{}^{R}{}_{30}$, and HIV-$1_{DRV}{}^{R}{}_{40}$ and were treated with various concentrations of each inhibitor. These DRV-resistant HIV-$1_{DRV}{}^{R}{}_{S}$ variants are highly resistant to all current clinically used PIs including DRV and nucleoside/nucleotide reverse transcriptase inhibitors such as tenofovir. IC_{50} values were determined using p24 assay.[33,34] The results are shown in Table 2. Oxazole derivative **3g** was less potent against HIV_{NL4-3} than DRV (3.4 nM vs. 22 nM). Its fold-change against $HIV_{DRV}{}^{R}{}_{P20}$ is similar to that of DRV, however, fold-changes against $HIV_{DRV}{}^{R}{}_{P30}$ and $HIV_{DRV}{}^{R}{}_{P40}$ were more than 3- and 6-fold lower than DRV (fold differences for DRV 71- and >297-fold). Inhibitor **3h** with a hydroxymethyl side chain on the oxazole ring showed similar IC_{50} values as DRV against HIV_{NL4-3}. Its fold-change of antiviral activity against $HIV_{DRV}{}^{R}{}_{20}$ was higher than compound **3g** and DRV, although the fold-changes against $HIV_{DRV}{}^{R}{}_{P30}$ and $HIV_{DRV}{}^{R}{}_{P40}$ were similar to DRV. This data indicates an interesting profile for the novel inhibitor **3g** toward DRV-resistant variants, and is to be considered a starting point for further optimization.

X-ray crystal structure description

To gain molecular insight into interactions of the oxazole inhibitors, we co-crystallized inhibitor **3g** (GRL-5311) with wild-type HIV-1 protease and the X-ray structure was refined at 1.30 Å resolution to an R_{work}/R_{free} of 15.4/19.6 % (PDB ID: 6B4N). The structure contains HIV-1 protease dimer with inhibitor **3g** bound in a single orientation. The HIV-1 protease dimer structure closely resembles our reported structure of protease-DRV complex with RMSD of 0.22 Å for all Cα atoms.[20] Larger differ ences between the corresponding Cα atoms are evident in one subunit of the dimer, where the differences of 0.75 Å occurred for residues 53′ to 54′ in the flap region and 0.77 Å for residues 80′ and 81′ in the 80s loop. These shifts are probably because the inhibitor **3g** has a larger P2′ and P3′ substituted oxazole group relative to the P2′ ligand of DRV. The inhibitor binds in the active site showing similar interactions for P2-*bis*-THF, the urethane functionality, and the P1-phenylmethyl side chain to those observed for the HIV-1 protease-DRV X-ray structure.[20]

The major differences for inhibitor **3g** interactions with HIV-1 protease are evident in the S2′ subsite where the 4-amino group of DRV was replaced by a substituted oxazole group. As shown in Figure 3, the oxazole nitrogen forms a strong hydro gen bond with the backbone NH of Asp30′. Interestingly, the carboxyl group of the ester side chain also forms a strong hydrogen bond with the Asp30′ backbone NH. The oxygen atom of the oxazole heterocycle forms a water-mediated interaction with Gly48′ amide NH. The carbonyl group of the oxazole side chain has two orientations and both stack against the carbox-ylic acid side chain of Asp30′. In one *S-trans* orientation of the ester, the methoxy oxygen is within hydrogen bonding distance of the Lys45′ amine side chain. Furthermore, the aromatic P2′ ring in **3g** has shifted toward the flap region, as shown in the overlay of X-ray structures of DRV-bound HIV-1 protease and inhibitor **3g**-bound HIV-1 protease (Figure 4). The side chain of Asp30′ has also shifted toward Asn88 to accommodate the oxazole ring. This heterocyclic core shows good van der Waals interactions with the side chains of Ile47′, Asp29′, and the main chain of Gly48′. These interactions may be responsible for the inhibitor′s high affinity for HIV-1 protease.

Conclusions

In conclusion, we have designed, synthesized, and examined a number of HIV-1 PIs containing carboxylic acid derivatives and substituted oxazole derivatives as P2′ ligands. These ligands are designed to enhance interactions with backbone atoms and residue in the S2′ subsite. Inhibitor **3b** with 4-carboxamide functionality showed enhanced potency over the carboxylic acid **3a**. The X-ray structure of **3b**-bound HIV-1 protease showed key hydrogen bonding interactions with Asp30′ backbone NH. Furthermore, the carboxamide also formed an interesting water-mediated hydrogen bond with the Gly48′ carbonyl group. Antiviral activity of **3b** showed that it is highly active against HIV_{AO2} with EC_{50} value of 29 nM. Antiviral activity of **3b** against HIV-2_{ROD} or $HIV_{DRV}{}^{R}{}_{P20}$ was 30 nM and 97 nM. There was only 2.6-fold increase in its EC_{50} value relative to its EC_{50} against HIV_{WT}. Based on the X-ray structure of **3b**-bound HIV-1 protease and its biological properties, we have examined a series of derivatives, including stereochemically defined alcohols, a ketone, a methoxymethylamide, 2-phenyl oxazole derivatives, and 5-phenyl oxazole derivatives. Both methyl ketone **3d** and its reduced products provided very potent enzyme inhibitory and antiviral activity similar to DRV. Various oxazole derivatives also displayed very potent antiviral activity. In particular, inhibitors **3g** and **3h** with 2-phenyloxazoles as the P2′ ligands showed very potent antiviral activity. While inhibitor **3h** has shown 10-fold better IC_{50} value than inhibitor **3g** against HIVNL4-3, inhibitor **3h** also showed similar fold-changes as DRV against $HIV_{DRV}{}^{R}{}_{P30}$ and $HIV_{DRV}{}^{R}{}_{40}$. However, its fold-changes are higher against $HIV_{DRV}{}^{R}{}_{P20}$. While inhibitor **3g** showed an IC_{50} value of 22 nM against HIVNL4-3, its fold-changes against DRV-resistant viruses are superior to inhibitor **3h** or DRV. The X-ray crystal structure of **3g**-bound HIV-1 protease revealed several new hydrogen bonds and water-mediated hydrogen bonding interactions in the S2′ subsite of HIV-1 protease. Further design and synthesis of new inhibitors using this molecular insight is in progress.

Experimental Section

General

All moisture-sensitive reactions were carried out in an oven dried flask under argon atmosphere. All chemicals and reagents were purchased from commercial suppliers and used without further purification. Anhydrous solvents were obtained as follows: anhydrous tetrahydrofuran, diethyl ether, and benzene were distilled from sodium metal under argon. Anhydrous dichloromethane, toluene, methanol, and acetonitrile were dried via distillation from CaH_2 under argon. All other solvents were HPLC grade. ^{1}H NMR and ^{13}C NMR spectra were recorded on Varian INOVA300-1, Bruker Avance ARX-400 and Bruker DRX-500 spectrometers. NMR data are reported as: δ value (chemical shift, *J*-value (Hz), integration, where s=singlet, d=doublet, t=triplet, q=quartet, br= broad). Low resolution mass analyses were performed on a Agilent 1290 Infinity II spectrometer. High-resolution mass spectrometric analyses were performed at the Purdue University Campus-wide Mass Spectrometry Center. TLC analysis was carried out with SiliCycle 60A-F_{254} plates. Flash chromatography was performed using SiliCycle 230–400 mesh, 60 Å pore diameter silica gel. HPLC analysis was performed on a Agilent 1260 Infinity instrument. All test inhibitors showed purity >95% by HPLC analysis.

4-(*N*-((2*R*,3*S*)-3-((*tert*-Butoxycarbonyl)amino)-2-hydroxy-4-phenyl-butyl)-*N*-isobutylsulfamoyl)benzoic acid (7)

To a solution of compound **5** (81 mg, 0.156 mmol) in MeOH (14 mL) was added K_2CO_3 (113 mg, 0.392 mmol) and the reaction was stirred at 23°C for 1 h. The reaction mixture was concentrated under reduced pressure and the residue partitioned between water and EtOAc. The organic layers were dried over anhydrous sodium sulfate, filtered and concentrated. The crude was purified by silica gel flash chromatography (30% EtOAc in *n*-hexanes) providing *tert*-butyl ((2*S*,3*R*)-4-((4-formyl-*N*-isobutylphenyl)sulfonamido)-3-hydroxy-1-phenylbutan-2-yl)carbamate (98% yield). ^{1}H NMR (400 MHz, $CDCl_3$) δ=10.08 (s, 1H), 8.00 (d, *J*=8.4 Hz, 2H), 7.93 (d, *J*=8.3 Hz, 2H), 7.41–7.11 (m, 5H), 4.67 (d, *J*=8.2 Hz, 1H), 3.95–3.64 (m, 3H), 3.16 (d, *J*=5.8 Hz, 2H), 3.03–2.71 (m, 4H), 1.96–1.73 (m, 1H), 1.34 (s, 9H), 0.86 ppm (dd, *J*=8.8, 6.7 Hz, 6H). ^{13}C NMR (100 MHz, $CDCl_3$) δ=190.9, 156.4, 144.2, 138.9, 137.8, 130.3, 129.6, 128.7, 128.1, 127.8, 126.7, 80.1, 72.7, 58.1, 55.1, 53.2, 35.7, 28.4, 27.2, 20.2, 20.0 ppm. LRMS-ESI (*m*/*z*): 527.2 [*M*+Na]$^+$. This aldehyde intermediate (41 mg, 0.081 mmol) was dissolved in *t*BuOH (5 mL) and 2-methyl-2-butene (2 mL) was added at 23°C; 2.6 mL of a stock solution obtained by dissolving $NaH_2PO_4{\cdot}H_2O$ (600 mg) and $NaClO_2$ (600 mg) in 6 mL of water was added and the reaction mixture was stirred at 23°C for 50 min. Water (3 mL) was added and the reaction mixture was extracted with EtOAc. The organic layers were washed with brine, dried over anhydrous sodium sulfate, filtered and concentrated. The crude was purified by silica gel flash chromatography (5% to 10% MeOH in CH_2Cl_2) providing compound **7** as a white solid (95% yield). ^{1}H NMR (400 MHz, CD_3OD) δ=8.17 (d, *J*=8.3 Hz, 2H), 7.92 (d, *J*=8.3 Hz, 2H), 7.30–7.18 (m, 3H), 7.18–7.09 (m, 2H), 3.71 (t, *J*=7.1 Hz, 1H), 3.64–3.53 (m, 1H), 3.42 (dd, *J*=15.0, 1.9 Hz, 1H), 3.20–3.01 (m, 2H), 2.94 (dd, *J*=13.7, 6.7 Hz, 1H), 2.54 (dd, *J*=13.7, 10.8 Hz, 1H), 2.10–1.95 (m, 1H), 1.36–1.21 (m, 9H), 0.89 ppm (dd, *J*=15.4, 6.6 Hz, 6H). ^{13}C NMR (100 MHz, DMSO) δ=168.3, 158.1, 144.9, 140.3, 135.8, 131.5, 130.6, 129.3, 128.7, 127.2, 80.2, 74.0,

58.3, 57.0, 53.6, 37.4, 28.8, 27.9, 20.5 ppm. LRMS-ESI (*m*/*z*): 521.2 [*M*+H]$^+$, 543.1 [*M*+Na]$^+$.

tert-Butyl ((2*S*,3*R*)-3-hydroxy-4-((*N*-isobutyl-4-(methoxy(methyl)-carbamoyl)phenyl)sulfonamido)-1-phenylbutan-2-yl)carbamate (8)

Compound **7** (58 mg, 0.111 mmol) was dissolved in dry CH_2Cl_2 (6 mL) and *N*-methyl morpholine (27 μL, 0.244 mmol) was added. The solution was cooled to −15°C and *i*BuOCOCl (16 μL, 0.122 mmol) was added. The reaction mixture was stirred at −15°C for 15 min, then *N*,*O*-dimethylhydroxylamine hydrochloride (11 mg, 0.113 mmol) was added and the reaction was stirred at 23°C for 12 h. The mixture was then partitioned between water and CH_2Cl_2. Organic layer was dried over anhydrous sodium sulfate, filtered and concentrated. The crude was purified by silica gel flash chromatography (5% MeOH in CH_2Cl_2) providing compound **8** as a white solid (76% yield). ^{1}H NMR (400 MHz, $CDCl_3$) δ=7.99–7.70 (m, 4H), 7.39–7.10 (m, 5H), 4.69 (d, *J*=7.6 Hz, 1H), 3.96–3.68 (m, 3H), 3.51 (s, 3H), 3.37 (s, 3H), 3.13 (d, *J*=5.7 Hz, 2H), 3.05–2.80 (m, 4H), 1.94–1.75 (m, 1H), 1.46–1.20 (m, 9H), 0.86 ppm (dd, *J*=11.1, 6.6 Hz, 6H). ^{13}C NMR (100 MHz, $CDCl_3$) δ=168.3, 156.3, 140.5, 138.4, 138.0, 129.7, 129.0, 128.6, 127.2, 126.6, 79.9, 72.8, 61.5, 58.4, 55.1, 53.6, 35.6, 33.4, 28.4, 27.2, 20.2, 20.0 ppm. LRMS-ESI (*m*/*z*): 564.3 [*M*+H]$^+$, 586.2 [*M*+Na]$^+$.

Methyl 2-(4-(*N*-((2*R*,3*S*)-3-((*tert*-butoxycarbonyl)amino)-2-hy-droxy-4-phenylbutyl)-*N*-isobutylsulfamoyl)phenyl)oxazole-4-car-boxylate (9)

Compound **7** (32 mg, 0.0615 mmol) was dissolved in dry DMF (4 mL) and the solution was cooled to 0°C. EDCI (14 mg, 0.074 mmol), HOBt (10 mg, 0.074 mmol), *N*,*N*-DIPEA (20 mL, 0.153 mmol) and DL-serine methyl ester hydrochloride (12 mg, 0.074 mmol) were sequentially added to the solution and the reaction mixture was stirred at 23°C for 16 h. Water was added and the reaction mixture was extracted with EtOAc. Organic layers were dried over anhydrous sodium sulfate, filtered and concentrated. The crude was purified by silica gel flash chromatography (EtOAc) providing methyl (4-(*N*-((2*R*,3*S*)-3-((*tert*-butoxycarbonyl)amino)-2-hydroxy-4-phenylbutyl)-*N*-isobutylsulfamoyl)benzoyl)serinate as a colorless oil (91% yield). ^{1}H NMR (400 MHz, $CDCl_3$) δ=7.94 (d, *J*=8.4 Hz, 2H), 7.83 (d, *J*=8.3 Hz, 2H), 7.42–7.13 (m, 5H), 4.88 (dt, *J*=7.0, 3.3 Hz, 1H), 4.67 (d, *J*=8.1 Hz, 1H), 4.08–4.00 (m, 2H), 3.92– 3.86 (m, 1H), 3.86–3.68 (m, 5H), 3.13 (d, *J*=5.7 Hz, 2H), 3.04–2.82 (m, 4H), 2.63 (br, 1H), 1.92–1.78 (m, 1H), 1.67 (s, 1H), 1.65–1.51 (m, 1H), 1.34 (s, 9H), 0.87 ppm (dd, *J*=10.6, 6.6 Hz, 6H). The above intermediate (70 mg, 0.113 mmol) was dissolved in dry CH_2Cl_2 (5 mL) and the solution was cooled to −78°C. DAST (17 μL, 0.124 mmol) was added dropwise. The reaction mixture was stirred at −78°C for 30 min (TLC monitoring in 100% EtOAc) and then quenched with K_2CO_3 and passed quickly through a silica gel column pretreated with triethylamine and eluted with EtOAc. The crude material recovered from the column was dried under reduced pressure and dissolved in dry CH_2Cl_2 (5 mL) and the resulting solution was cooled to 0°C. $BrCCl_3$ (13 μL, 0.124 mmol) and DBU (19 μL, 0.124 mmol) were sequentially added and the reaction mixture was then stirred at 23°C for 2.5 h. Solvents were evaporated under reduced pressure and the residue was purified by silica gel flash chromatography (50% EtOAc in *n*-hexane) providing compound **9** as a white solid (64% yield over two steps). ^{1}H NMR (400 MHz, $CDCl_3$) δ=8.35 (s, 1H),

8.24 (d, *J*=8.5 Hz, 2H), 7.87 (d, *J*=8.5 Hz, 2H), 7.40–7.16 (m, 5H), 4.67 (d, *J*=7.7 Hz, 1H), 3.97 (s, 3H), 3.94–3.86 (m, 1H), 3.86–3.70 (m, 2H), 3.16 (d, *J*=5.8 Hz, 2H), 3.08–2.83 (m, 4H), 1.94–1.80 (m, 1H), 1.34 (s, 9H), 0.86 ppm (dd, *J*=11.0, 6.6 Hz, 6H). 13C NMR (100 MHz, $CDCl_3$) δ=161.5, 160.9, 156.3, 144.7, 141.2, 137.9, 135.1, 130.2, 129.7, 128.7, 128.0, 127.6, 126.7, 108.9, 80.0, 72.8, 58.3, 55.1, 53.3, 52.6, 35.6, 28.4, 27.2, 20.2, 20.0 ppm. LRMS-ESI (*m*/*z*): 624.2 $[M+Na]^+$, 502.1 $[M-Boc+H]^+$.

tert-Butyl ((2*S*,3*R*)-3-hydroxy-4-((*N*-isobutyl-4-(oxazol-5-yl)phe-nyl)sulfonamido)-1-phenylbutan-2-yl)carbamate (10)

Compound **5** (52 mg, 0.086 mmol) and TosMIC (40 mg, 0.206 mmol) were dissolved in MeOH (3 mL) in a sealed tube and K_2CO_3 (76 mg, 0.548 mmol) was added. The reaction mixture was stirred at 55°C for 1.5 h (TLC monitoring). The reaction mixture was then cooled to room temperature and filtered on a Celite pad. The crude residue was purified by silica gel flash chromatography (20% to 50% EtOAc in *n*-hexane) providing compound **10** as a white solid (96% yield). ^{1}H NMR (500 MHz, $CDCl_3$) δ=8.04 (s, 1H), 7.88 (d, *J*=8.5 Hz, 2H), 7.82 (d, *J*=8.4 Hz, 2H), 7.55 (s, 1H), 7.45–7.18 (m, 5H), 4.81 (d, *J*=8.4 Hz, 1H), 3.96–3.75 (m, 2H), 3.32–3.16 (m, 2H), 3.12–2.80 (m, 4H), 1.98–1.81 (m, 1H), 1.35 (s, 9H), 0.93 ppm (dd, *J*=11.2, 6.6 Hz, 6H). ^{13}C NMR (125 MHz, $CDCl_3$) δ=156.3, 151.6, 150.0, 138.4, 137.9, 131.7, 129.6, 128.6, 128.2, 126.6, 124.9, 124.0, 79.9, 72.8, 58.4, 54.9, 53.5, 35.6, 28.4, 27.2, 20.2, 20.0 ppm.

tert-Butyl ((2*S*,3*R*)-4-((4-(2-acetyloxazol-5-yl)-*N*-isobutylphenyl)-sulfonamido)-3-hydroxy-1-phenylbutan-2-yl)carbamate (11)

Compound **10** (42 mg, 0.0775 mmol) was dissolved in dry THF (2 mL) and the resulting solution was cooled to −15°C. Then *i*PrMgCl (2.0M solution in THF, 116 μL, 0.232 mmol) was added dropwise and the mixture was stirred for 40 min at −15°C. *N*-Me-thoxy-*N*-methylacetamide (25 μL, 0.232 mmol) was added and the reaction mixture was allowed to slowly reach 23°C and stirred for 5 h. The reaction was quenched with a saturated solution of NH_4Cl and extracted with EtOAc. The organic layers were dried over anhydrous sodium sulfate, filtered and concentrated. The crude was purified by silica gel flash chromatography (20% to 50% EtOAc in *n*-hexane) providing compound **11** as an amorphous white solid (79% yield). ^{1}H NMR (400 MHz, $CDCl_3$) δ=7.65 (s, 1H), 7.40–7.14 (m, 5H), 4.62 (br, 1H), 3.97–3.66 (m, 3H), 3.16 (d, *J*=5.6 Hz, 2H), 3.06–2.83 (m, 4H), 2.72 (s, 3H), 1.96–1.79 (m, 1H), 1.35 (s, 9H), 0.88 (dd, *J*=11.1, 6.7 Hz, 6H), 8.01–7.79 ppm (m, 4H).

4-(*N*-((2*R*,3*S*)-3-(((((3*R*,3a*S*,6a*R*)-Hexahydrofuro[2,3-*b*]furan-3-yl)oxy)carbonyl)amino)-2-hydroxy-4-phenylbutyl)-*N*-isobutylsul-famoyl)benzoic acid (3a)

Compound **7** (11.5 mg, 0.0221 mmol) was dissolved in dry CH_2Cl_2 (3 mL) and TFA (400 μL) was added. The resulting mixture was stirred at 23°C for 3 h. Solvents were evaporated under reduced pressure, then CH_2Cl_2 (5 mL) was added and evaporated twice to provide the corresponding Boc-deprotected compound, which was carried on without further purification. The compound was dissolved in a mixture of MeCN (4 mL) and water (0.4 mL), then *N*,*N*-DIPEA (39 μL, 0.221 mmol) and activated *bis*-THF carbonate **6** (7.8 mg, 0.0252 mmol) were sequentially added and the reaction mixture was stirred at 23°C for 3

days. Volatiles were evaporated under reduced pressure and the crude residue was purified by HPLC to provide pure **3a** as a white solid (89% yield over two steps). ^{1}H NMR (500 MHz, CD_3OD) δ=8.22 (d, *J*=8.4 Hz, 2H), 7.97 (d, *J*=8.4 Hz, 2H), 7.35–7.24 (m, 4H), 7.24–7.13 (m, 1H), 5.62 (d, *J*=5.2 Hz, 1H), 3.97 (dd, *J*=9.7, 6.0 Hz, 1H), 3.85–3.74 (m, 4H), 3.74–3.63 (m, 1H), 3.55–3.47 (m, 1H), 3.27–3.17 (m, 2H), 3.08 (dd, *J*=15.0, 8.3 Hz, 1H), 2.98 (dd, *J*=13.7, 6.7 Hz, 1H), 2.94–2.86 (m, 1H), 2.55 (dd, *J*=13.8, 10.9 Hz, 1H), 2.14–2.00 (m, 1H), 1.59–1.46 (m, 1H), 1.41–1.28 (m, 1H), 0.94 ppm (dd, *J*=26.3, 6.6 Hz, 6H). 13C NMR (125 MHz, CD_3OD) δ=167.2, 156.7, 143.7, 139.2, 130.5, 129.5, 128.3, 127.6, 126.3, 109.8, 73.6, 73.2, 71.1, 69.7, 57.4, 56.5, 52.5, 45.9, 36.1, 26.9, 26.0, 19.4 ppm.

(3*R*,3a*S*,6a*R*)-Hexahydrofuro[2,3-*b*]furan-3-yl ((2*S*,3*R*)-4-((4-carba-moyl-*N*-isobutylphenyl)sulfonamido)-3-hydroxy-1-phenylbutan-2-yl)carbamate (3b)

Compound **3a** (3.4 mg, 0.0059 mmol) was dissolved in THF (4 mL) and pyridine (0.5 mL), Boc_2O (2 mg, 0.0092 mmol) and $(NH_4)_2CO_3$ (1 mg, 0.0104 mmol) were sequentially added. The reaction mixture was stirred at 23°C for 14 h and then concentrated under reduced pressure. The residue was purified by silica gel flash chromatography (10% MeOH in CH_2Cl_2) providing **3b** as a white solid (76% yield). ^{1}H NMR (400 MHz, $CDCl_3$) δ=7.95 (d, *J*=8.4 Hz, 2H), 7.84 (d, *J*=8.3 Hz, 2H), 7.36–7.12 (m, 5H), 6.34 (br, 1H), 5.82 (br, 1H), 5.64 (d, *J*=5.2 Hz, 1H), 5.03–4.87 (m, 2H), 3.98–3.79 (m, 4H), 3.76–3.58 (m, 2H), 3.51–3.41 (m, 1H), 3.21–3.02 (m, 2H), 3.00–2.84 (m, 3H), 2.78 (dd, *J*=13.9, 9.0 Hz, 1H), 1.85 (dt, *J*=13.6, 6.6 Hz, 1H), 1.74–1.56 (m, 2H), 1.55–1.42 (m, 1H), 0.90 ppm (dd, *J*=9.5, 6.6 Hz, 6H). LRMS-ESI (*m*/*z*): 576.3 $[M+H]^+$, 598.2 $[M+Na]^+$; HRMS-ESI (*m*/*z*) $[M+Na]^+$ calculated for $C_{28}H_{37}N_3O_8SNa$ 598.2199, found 598.2206.

(3*R*,3a*S*,6a*R*)-Hexahydrofuro[2,3-*b*]furan-3-yl ((2*S*,3*R*)-3-hydroxy-4-((*N*-isobutyl-4-(methoxy(methyl)carbamoyl)phenyl)sulfonami-do)-1-phenylbutan-2-yl)carbamate (3c)

Compound **8** (6.5 mg, 0.0115 mmol) was dissolved in dry CH_2Cl_2 (3 mL) and TFA (200 μL) was added to the solution. The reaction mixture was stirred at 23°C for 2 h. Solvents were evaporated under reduced pressure, then CH_2Cl_2 (5 mL) was added and evaporated twice to provide the corresponding Boc-deprotected compound, which was carried on without further purification. The compound was dissolved in MeCN (4 mL), then *N*,*N*-DIPEA (20 μL, 0.115 mmol) and activated *bis*-THF carbonate **6** (3.4 mg, 0.0115 mmol) were sequentially added and the reaction mixture was stirred at 23°C for 5 days. Volatiles were evaporated under reduced pressure and the residue was purified by silica gel flash chromatography (50% EtOAc in *n*-hexane) to provide **3c** as a white solid (73% yield over two steps). ^{1}H NMR (400 MHz, $CDCl_3$) δ=7.87–7.75 (m, 4H), 7.39–7.11 (m, 5H), 5.64 (d, *J*=5.2 Hz, 1H), 5.03 (dd, *J*=14.0, 6.2 Hz, 1H), 4.92 (d, *J*= 8.5 Hz, 1H), 4.00–3.80 (m, 4H), 3.75–3.62 (m, 2H), 3.59–3.47 (m, 4H), 3.39 (s, 3H), 3.21 (dd, *J*=15.0, 8.5 Hz, 1H), 3.14–2.96 (m, 3H), 2.95–2.71 (m, 3H), 1.93–1.78 (m, 1H), 1.50–1.38 (m, 2H), 0.90 ppm (dd, *J*=20.8, 6.6 Hz, 6H).

(3*R*,3a*S*,6a*R*)-Hexahydrofuro[2,3-*b*]furan-3-yl ((2*S*,3*R*)-4-((4-acetyl-*N*-isobutylphenyl)sulfonamido)-3-hydroxy-1-phenylbutan-2-yl)-carbamate (3d)

Compound **8** (35 mg, 0.062 mmol) was dissolved in dry THF (2.5 mL) and the resulting solution was cooled to −78°C. MeMgBr (3M solution in Et_2O, 105 μL, 0.310 mmol) was

added dropwise and the reaction mixture was stirred at −78°C for 4 h and then quenched with a saturated solution of NH_4Cl. The mixture was extracted with EtOAc and the organic layers were dried over anhydrous sodium sulfate, filtered and concentrated. The crude was purified by silica gel flash chromatography (50% EtOAc in *n*-hexanes) providing *tert*-butyl ((2*S*,3*R*)-4-((4-acetyl-*N*-iso-butylphenyl)sulfonamido)-3-hydroxy-1-phenylbutan-2-yl)carbamate (98% yield). ^{1}H NMR (400 MHz, $CDCl_3$) δ=8.07 (d, *J*=8.3 Hz, 2H), 7.88 (d, *J*=8.3 Hz, 2H), 7.37–7.14 (m, 5H), 4.70 (d, *J*=7.5 Hz, 1H), 3.92 (br, 1H), 3.86–3.69 (m, 2H), 3.23–3.12 (m, 2H), 3.07–2.82 (m, 4H), 2.66 (s, 3H), 1.97–1.72 (m, 2H), 1.36 (s, 9H), 0.89 ppm (dd, *J*= 9.9, 6.6 Hz, 6H). 13C NMR (100 MHz, $CDCl_3$) δ=196.89, 156.37, 142.78, 140.14, 137.86, 129.65, 129.10, 128.69, 127.77, 126.68, 80.05, 72.71, 58.30, 55.08, 53.35, 35.68, 28.39, 27.21, 27.01, 20.20, 20.01 ppm. The above methyl ketone intermediate was then Boc-deprotected and submitted to coupling with the activated *bis*-THF derivative **6** as described for compound **3c**, providing pure compound **3d** as an amorphous white solid (78% yield over two steps). ^{1}H NMR (400 MHz, $CDCl_3$) δ=8.08 (d, *J*=8.4 Hz, 2H), 7.87 (d, *J*=8.4 Hz, 2H), 7.35–7.15 (m, 5H), 5.65 (d, *J*=5.2 Hz, 1H), 5.02 (dd, *J*=14.0, 6.2 Hz, 1H), 4.92 (d, *J*=8.3 Hz, 1H), 4.01–3.81 (m, 4H), 3.76–3.62 (m, 2H), 3.55 (br, 1H), 3.26–3.14 (m, 1H), 3.13–2.96 (m, 3H), 2.96–2.74 (m, 3H), 2.66 (s, 3H), 1.92–1.75 (m, 1H), 1.74–1.40 (m, 2H), 0.90 ppm (dd, *J*=19.9, 6.6 Hz, 6H). LRMS-ESI (*m*/*z*): 597.1 [*M*+Na]$^+$; HRMS-ESI (*m*/*z*) [*M*+Na]$^+$ calculated for $C_{29}H_{38}N_2O_8SNa$ 597.2247, found 597.2243.

(3*R*,3a*S*,6a*R*)-Hexahydrofuro[2,3-*b*]furan-3-yl ((2*S*,3*R*)-3-hydroxy-4-((4-((*R*)-1-hydroxyethyl)-*N*-isobutylphenyl)sulfonamido)-1-phe-nylbutan-2-yl)carbamate (3e)

Compound **3d** (3 mg, 0.0052 mmol) was dissolved in dry CH_2Cl_2 (0.5 mL) and Et_3N (280 μL) and HCO_2H (140 μL) were added at 0°C. After stirring for 30 min, Noyori asymmetric transfer hydrogenation catalyst RuCl[(*R*,*R*)-TsDPEN](mesity-lene) (0.5 mol%) was added and the reaction mixture was stirred at 23°C for 7 h. The reaction mixture was then quenched saturated $NaHCO_3$ and extracted with CH_2Cl_2. The organic layers were dried over anhydrous sodium sulfate, filtered and concentrated. The crude was purified by silica gel flash chromatography (20% to 60% EtOAc in *n*-hexane) providing **3e** as a white solid (94% yield). ^{1}H NMR (500 MHz, $CDCl_3$) δ=7.81 (d, *J*=8.3 Hz, 2H), 7.60 (d, *J*= 8.2 Hz, 2H), 7.41–7.21 (m, 5H), 5.70 (d, *J*=5.2 Hz, 1H), 5.11–4.93 (m, 3H), 4.04–3.97 (m, 1H), 3.96–3.84 (m, 3H), 3.80–3.66 (m, 2H), 3.27–3.11 (m, 2H), 3.11–3.00 (m, 2H), 3.00–2.79 (m, 3H), 1.96–1.82 (m, 1H), 1.77–1.65 (m, 1H), 1.58 (d, *J*=6.5 Hz, 3H), 1.55–1.46 (m, 1H), 0.98 ppm (dd, *J*=23.7, 6.6 Hz, 6H). ^{13}C NMR (125 MHz, $CDCl_3$) δ= 155.9, 151.7, 138.0, 137.2, 129.8, 129.0, 128.1, 127.1, 126.6, 109.7, 73.9, 73.3, 71.3, 70.0, 60.9, 59.4, 55.5, 54.3, 45.8, 36.1, 27.8, 26.3, 25.9, 20.6, 20.3 ppm. LRMS-ESI (*m*/*z*): 577.2 [*M*+H]$^+$, 599.3 [*M*+ Na]$^+$; HRMS-ESI (*m*/*z*) [*M*+Na]$^+$ calculated for $C_{29}H_{40}N_2O_8SNa$ 599.2404, found 599.2408. HPLC analysis: Chiralpak IA-3 column, 10% isopropanol in *n*-hexane, flow rate=1 mLmin^{-1}, *t*=24°C, l=254 nm, t_R=32.1 min, d.r. 98:2.

(3*R*,3a*S*,6a*R*)-Hexahydrofuro[2,3-*b*]furan-3-yl ((2*S*,3*R*)-3-hydroxy-4-((4-((*S*)-1-hydroxyethyl)-*N*-isobutylphenyl)sulfonamido)-1-phe-nylbutan-2-yl)carbamate (3f)

Compound **3f** was obtained from **3d** following the same procedure described for compound **3e** employing RuCl(*p*-cymene)[(*S*,*S*)-Ts-DPEN] as the catalyst. Compound **3f** was obtained in 98% yield. ^{1}H NMR (500 MHz, $CDCl_3$) δ=7.81 (d, *J*=8.2 Hz, 2H), 7.60 (d, *J*=8.1 Hz,

2H), 7.41–7.18 (m, 5H), 5.70 (d, *J*=5.2 Hz, 1H), 5.10–4.90 (m, 3H), 4.04–3.97 (m, 1H), 3.97–3.87 (m, 3H), 3.79–3.64 (m, 3H), 3.23 (dd, *J*=15.1, 8.5 Hz, 1H), 3.14 (dd, *J*=14.2, 3.8 Hz, 1H), 3.11–3.02 (m, 2H), 3.00–2.93 (m, 1H), 2.92–2.80 (m, 2H), 2.20 (br, 1H), 1.96–1.85 (m, 1H), 1.76–1.64 (m, 1H), 1.58 (d, *J*=6.5 Hz, 3H), 1.55–1.46 (m, 1H), 0.98 ppm (dd, *J*=24.1,6.6 Hz, 6H). 13C NMR (125 MHz, $CDCl_3$) δ=155.9, 151.6, 138.0, 137.3, 129.8, 129.0, 128.0, 127.1, 126.6, 109.7, 73.9, 73.3, 71.3, 70.0, 59.4, 55.6, 54.3, 45.8, 36.1, 28.3, 27.8, 26.3, 25.9, 20.6, 20.3 ppm. LRMS-ESI (*m*/*z*): 577.2 $[M+H]^+$, 599.2 $[M+Na]^+$; HRMS-ESI (*m*/*z*) $[M+Na]^+$ calculated for $C_{29}H_{40}N_2O_8SNa$ 599.2404, found 599.2408. HPLC analysis: Chiralpak IA-3 column, 10% isopropanol in *n*-hexane, flow rate=1 $mLmin^{-1}$, *t*=24°C, l=254 nm, t_R=34.6 min, d.r. 98:2.

Methyl 2-(4-(*N*-((2*R*,3*S*)-3-(((((3*R*,3a*S*,6a*R*)-hexahydrofuro[2,3-*b*]furan-3-yl)oxy)carbonyl)amino)-2-hydroxy-4-phenylbutyl)-*N*-isobutylsulfamoyl)phenyl)oxazole-4-carboxylate (3g)

Compound **3g** was obtained from compound **9** and activated *bis*-THF derivative **6** following the same procedure described for compound **3c** (61% yield over two steps). ^{1}H NMR (500 MHz, $CDCl_3$) δ=8.42 (s, 1H), 8.33 (d, *J*=8.5 Hz, 2H), 7.95 (d, *J*=8.5 Hz, 2H), 7.43–7.17 (m, 5H), 5.71 (d, *J*=5.2 Hz, 1H), 5.09 (dd, *J*=14.2, 6.3 Hz, 1H), 5.01 (d, *J*=8.4 Hz, 1H), 4.13–3.98 (m, 4H), 3.98–3.84 (m, 3H), 3.85–3.69 (m, 2H), 3.64 (s, 1H), 3.29 (dd, *J*=15.1, 8.3 Hz, 1H), 3.22–3.05 (m, 3H), 3.03–2.93 (m, 2H), 2.87 (dd, *J*=14.0, 9.1 Hz, 1H), 1.96–1.81 (m, 1H), 1.78–1.61 (m, 1H), 1.59–1.45 (m, 1H), 0.96 ppm (dd, *J*=25.2, 6.6 Hz, 6H). ^{13}C NMR (125 MHz, $CDCl_3$) δ=161.6, 160.9, 155.7, 144.8, 140.8, 137.7, 135.1, 130.4, 129.5, 128.8, 128.1, 127.7, 126.9, 109.5, 73.7, 72.9, 71.0, 69.8, 58.7, 55.4, 53.7, 52.7, 45.6, 35.8, 27.4, 26.0, 20.3, 20.0 ppm. LRMS-ESI (*m*/*z*): 658.2 $[M+H]^+$, 680.3 $[M+Na]^+$.

(3*R*,3a*S*,6a*R*)-Hexahydrofuro[2,3-*b*]furan-3-yl ((2*S*,3*R*)-3-hydroxy-4-((4-(4-(hydroxymethyl)oxazol-2-yl)-*N*-isobutylphenyl)sulfona-mido)-1-phenylbutan-2-yl)carbamate (3h)

Compound **9** (8.5 mg, 0.014 mmol) was dissolved in absolute EtOH (3 mL) and the resulting solution was cooled to 0°C. $NaBH_4$ (1.6 mg, 0.042 mmol) was added and the reaction mixture was stirred at 23°C for 24 h. The reaction was quenched with saturated aqueous NH_4Cl and extracted with EtOAc. The organic layers were dried over anhydrous sodium sulfate, filtered and concentrated. The crude was purified by silica gel flash chromatography (60% EtOAc in *n*-hexanes) providing the corresponding alcohol derivative (65% yield). This intermediate underwent Boc-deprotection and coupling with the *bis*-THF derivative **6** as described for compound **3c** (60% yield over two steps). ^{1}H NMR (500 MHz, $CDCl_3$) δ=8.17 (d, *J*=8.5 Hz, 2H), 7.86 (d, *J*=8.6 Hz, 2H), 7.73 (s, 1H), 7.36–7.11 (m, 5H), 5.64 (d, *J*=5.2 Hz, 1H), 5.01 (dd, *J*=14.2, 6.3 Hz, 1H), 4.94 (d, *J*=8.5 Hz, 1H), 4.70 (s, 2H), 3.96 (dd, *J*=9.6, 6.3 Hz, 1H), 3.94–3.77 (m, 3H), 3.78–3.61 (m, 3H), 3.56 (s, 1H), 3.20 (dd, *J*=15.2, 8.4 Hz, 1H), 3.14–2.98 (m, 3H), 2.96–2.84 (m, 2H), 2.84–2.74 (m, 1H), 1.91–1.79 (m, 1H), 1.71–1.53 (m, 1H), 1.52–1.41 (m, 1H), 0.98–0.84 ppm (m, 6H). ^{13}C NMR (125 MHz, $CDCl_3$) δ=160.5, 155.7, 142.4, 139.9, 137.7, 136.4, 131.4, 129.5, 128.8, 128.1, 127.2, 126.9, 109.5, 73.7, 72.9, 70.9, 69.8, 58.8, 57.3, 55.4, 53.7, 45.5, 35.8, 27.4, 26.0, 20.3, 20.1 ppm. LRMS-ESI (*m*/*z*): 630.3 $[M+H]^+$, 652.2 $[M+Na]^+$.

(3*R*,3a*S*,6a*R*)-Hexahydrofuro[2,3-*b*]furan-3-yl ((2*S*,3*R*)-3-hydroxy-4-((*N*-isobutyl-4-(oxazol-5-yl)phenyl)sulfonamido)-1-phenylbu-tan-2-yl)carbamate (3i)

Compound **3i** was obtained from compound **10** and activated *bis*-THF derivative **6** following the same procedure described for compound **3c** (47% over two steps). ^{1}H NMR (500 MHz, $CDCl_3$) δ=8.00 (s, 1H), 7.84 (d, *J*=8.7 Hz, 2H), 7.80 (d, *J*=8.6 Hz, 2H), 7.52 (s, 1H), 7.33–7.26 (m, 2H), 7.25–7.17 (m, 3H), 5.64 (d, *J*=5.2 Hz, 1H), 5.09–4.95 (m, 2H), 4.01–3.79 (m, 4H), 3.79–3.54 (m, 3H), 3.20 (dd, *J*=15.1, 8.4 Hz, 1H), 3.14–2.96 (m, 3H), 2.96–2.87 (m, 2H), 2.86–2.70 (m, 1H), 1.93–1.78 (m, 1H), 1.74–1.56 (m, 1H), 1.50–1.39 (m, 1H), 0.90 ppm (dd, *J*=22.2, 6.6 Hz, 6H). ^{13}C NMR (125 MHz, $CDCl_3$) δ=155.4, 151.4, 149.6, 137.7, 137.4, 131.7, 129.2, 128.5, 128.0, 126.5, 124.7, 123.9, 109.2, 73.4, 72.7, 70.7, 69.5, 58.5, 55.1, 53.5, 45.3, 35.5, 27.1, 25.7, 20.0, 19.7 ppm. LRMS-ESI (*m*/*z*): 600.3 $[M+H]^+$, 622.2 $[M+Na]^+$; HRMS-ESI (*m*/*z*) $[M+Na]^+$ calculated for $C_{30}H_{37}N_3O_8SNa$ 622.2199, found 622.2205.

(3*R*,3a*S*,6a*R*)-Hexahydrofuro[2,3-*b*]furan-3-yl ((2*S*,3*R*)-4-((4-(2-ace-tyloxazol-5-yl)-*N*-isobutylphenyl)sulfonamido)-3-hydroxy-1-phe-nylbutan-2-yl)carbamate (3j)

Compound **3j** was obtained from compound **11** and activated *bis*-THF derivative **6** following the same procedure described for compound **3c** (80% over two steps). ^{1}H NMR (500 MHz, $CDCl_3$) δ=7.92 (d, *J*=8.4 Hz, 2H), 7.86 (d, *J*=8.5 Hz, 2H), 7.66 (s, 1H), 7.35–7.26 (m, 3H), 7.26–7.17 (m, 2H), 5.64 (d, *J*=5.2 Hz, 1H), 5.01 (dd, *J*=14.0, 6.1 Hz, 1H), 5.00–4.92 (m, 1H), 4.00–3.80 (m, 4H), 3.75–3.62 (m, 2H), 3.59 (s, 1H), 3.21 (dd, *J*=15.2, 8.4 Hz, 1H), 3.15–2.97 (m, 3H), 2.95–2.85 (m, 2H), 2.80 (dd, *J*=13.8, 9.2 Hz, 1H), 2.72 (s, 3H), 1.85 (dt, *J*=13.3, 6.8 Hz, 1H), 1.73–1.56 (m, 1H), 1.51–1.39 (m, 1H), 0.90 ppm (dd, *J*=22.9, 6.6 Hz, 6H). ^{13}C NMR (125 MHz, $CDCl_3$) δ=185.6, 158.0, 155.8, 152.4, 139.5, 137.6, 130.9, 129.5, 128.8, 128.4, 126.9, 126.1, 126.0, 109.5, 73.8, 72.9, 71.0, 69.8, 58.7, 55.4, 53.7, 45.6, 35.8, 27.4, 26.9, 26.0, 20.3, 20.0 ppm. LRMS-ESI (*m*/*z*): 664.2 $[M+Na]^+$; HRMS-ESI (*m*/*z*) $[M+Na]^+$ calculated for $C_{32}H_{39}N_3O_9SNa$ 664.2305, found 664.2314.

(3*R*,3a*S*,6a*R*)-Hexahydrofuro[2,3-*b*]furan-3-yl ((2*S*,3*R*)-3-hydroxy-4-((4-(2-((*R*)-1-hydroxyethyl)oxazol-5-yl)-*N*-isobutylphenyl)sulfo-namido)-1-phenylbutan-2-yl)carbamate (3k)

Compound **3k** was obtained from compound **3j** following the same procedure described for compound **3e** (97% yield). ^{1}H NMR (400 MHz, $CDCl_3$) δ=7.93–7.63 (m, 4H), 7.43 (s, 1H), 7.35–7.04 (m, 5H), 5.64 (d, *J*= 5.2 Hz, 1H), 5.13–4.87 (m, 3H), 4.02–3.75 (m, 4H), 3.76–3.35 (m, 4H), 3.29–2.95 (m, 4H), 2.96–2.58 (m, 4H), 1.93–1.81 (m, 1H), 1.69 (d, *J*=6.7 Hz, 3H), 0.90 ppm (dd, *J*=15.4, 6.5 Hz, 6H). ^{13}C NMR (125 MHz, $CDCl_3$) δ=166.7, 157.4, 155.4, 137.7, 135.9, 131.8, 129.2, 128.8, 128.5, 128.0, 127.9, 126.5, 124.5, 124.0, 109.2, 78.5, 73.4, 70.9, 69.8, 69.5, 63.7, 58.5, 55.8, 53.4, 46.4, 35.8, 29.6, 27.1, 25.7, 21.3, 20.0, 19.9 ppm. LRMS-ESI (*m*/*z*): 644.4 $[M+H]^+$, 666.4 $[M+Na]^+$. HPLC analysis: Chiralpak IC column, 75% isopropanol in *n*-hexane, flow rate=0.8 mLmin^{-1}, *t*=24°C, l=254 nm, t_R=13.8 min, d.r. >99:1.

(3*R*,3a*S*,6a*R*)-Hexahydrofuro[2,3-*b*]furan-3-yl ((2*S*,3*R*)-3-hydroxy-4-((4-(2-((*S*)-1-hydroxyethyl)oxazol-5-yl)-*N*-isobutylphenyl)sulfon-amido)-1-phenylbutan-2-yl)carbamate (3l)

Compound **3l** was obtained from compound **3j** following the same procedure described for compound **3f** (95% yield). ^{1}H NMR (400 MHz, $CDCl_3$) δ=7.90–7.71 (m, 4H), 7.44 (s, 1H), 7.31–7.10 (m, 5H), 5.64 (d, *J*=5.2 Hz, 1H), 5.07–4.98 (m, 2H), 4.88–4.83 (m, 1H), 3.98–3.80 (m, 4H), 3.71–3.52 (m, 4H), 3.10–2.88 (m, 4H), 2.85–2.72 (m, 4H), 1.87– 1.79 (m, 1H), 1.68 (d, *J*=6.7 Hz, 3H), 0.91 ppm (dd, *J*=15.3, 6.5 Hz, 6H). ^{13}C NMR (125 MHz, $CDCl_3$) δ=166.7, 157.6, 155.4, 137.4, 135.8, 131.7, 129.2, 128.8, 128.5, 128.0, 127.4, 126.5, 124.5, 109.3, 78.5, 73.0, 70.8, 69.8, 69.5, 63.7, 58.4, 53.4, 46.5, 35.8, 29.5, 27.1, 24.8, 21.2, 20.0, 19.8 ppm. LRMS-ESI (*m*/*z*): 644.4 $[M+H]^+$, 666.3 $[M+Na]^+$. HPLC analysis: Chiralpak IC column, 75% isopropanol in *n*-hexane, flow rate=0.8 mLmin^{-1}, *t*=24°C, l=254 nm, t_R= 11.2 min, d.r. >99:1.

Determination of X-ray structure of HIV-1 protease and inhibitor 3g complex

The optimized HIV-1 protease was expressed and purified as described.[35] The protease–inhibitor complex was crystal-lized by the hanging drop vapor diffusion method with well solutions of 1.3M NaCl, 0.1M sodium acetate buffer (pH 5.5). Diffraction data were collected on a single crystal cooled to 90 K at SER-CAT (22-ID beamline), Advanced Photon Source, Argonne National Lab (Chicago, IL, USA) with X-ray wavelength of 0.8 Å, and processed by HKL-2000[36] with an *R*merge of 6.2%. Using the isomorphous structure[37] the crystal structure was solved by PHASER[38] in the CCP4i Suite[39–41] and refined in SHELX-97[42–44] with 1.3 Å resolution data. COOT[43,45] was used for manual modification of the atomic structure. PRODRG-2[46] was used to construct the inhibitor and the restraints for refinement. Alternative conformations were modeled, anisotropic atomic displacement parameters (*B* factors) were applied for all atoms including solvent molecules, and hydrogen atoms were added in the final round of refinement. The final refined solvent structure comprised two Na^+ ions, four Cl^- ions, and 234 water molecules. The crystallographic statistics are listed in a Table in the supporting information. The coordinates and structure factors of the PR with GRL-05311A (**3g**) structure have been deposited in the RCSB Protein Data Bank[47] with PDB ID: 6B4N.

Supplementary Material

Refer to Web version on PubMed Central for supplementary material.

Acknowledgments

This research was supported by the US National Institutes of Health (Grant GM53386 to A.K.G. and Grant GM62920 to I.T.W.). This work was also supported by the Intramural Research Program of the Center for Cancer Research, National Cancer Institute, National Institutes of Health, and in part by a Grant-in-Aid for Scientific Research (Priority Areas) from the Ministry of Education, Culture, Sports, Science, and Technology of Japan (Monbu-Kagakusho), a Grant for Promotion of AIDS Research from the Ministry of Health, Welfare, and Labor of Japan, and the Grant to the Cooperative Research Project on Clinical and Epidemiological Studies of Emerging and Reemerging Infectious Diseases (Renkei Jigyo) of Monbu-Kagakusho. The authors thank the Purdue University Center for Cancer Research, which supports the shared NMR and mass spectrometry facilities.

References

1. UNAIDS/WHO. AIDS Epidemic Update. Dec. 2006 http://data.u-naids.org/pub/report/2006/2006_gr_en.pdf
2. Greene WC. Eur J Immunol. 2007; 37:S94–S102. [PubMed: 17972351]
3. Sepkowitz KA. N Engl J Med. 2001; 344:1764–1772. [PubMed: 11396444]
4. Edmonds A, Yotebieng M, Lusiama J, Matumona Y, Kitetele F, Nap-ravnik S, Cole SR, Van Rie A, Behets F. PLoS Med. 2011:8e1001044.
5. Cohen MS, Chen YQ, McCauley M. N Engl J Med. 2011; 365:493–505. [PubMed: 21767103]
6. Dieffenbach CW, Fauci AS. Ann Intern Med. 2011; 154:766–771. [PubMed: 21628350]
7. Maartens G, Celum C, Lewin S. Lancet. 2014; 384:258–271. [PubMed: 24907868]
8. Cihlar T, Fordyce M. Curr Opin Virol. 2016; 18:50–56. [PubMed: 27023283]
9. Patel K, Hernµn MA, Williams PL, Seeger JD, McIntosh K, Van Dyke RB, Seage GR III. Clin Infect Dis. 2008; 46:507–515. [PubMed: 18199042]
10. Gupta R, Hill A, Sawyer AW, Pillay D. Clin Infect Dis. 2008; 47:712–722. [PubMed: 18662137]
11. Hue S, Gifford RJ, Dunn D, Fernhill E, Pillay D. J Virol. 2009; 83:2645–2654. [PubMed: 19158238]
12. Ghosh AK, Osswald HL, Prato G. J Med Chem. 2016; 59:5172–5208. [PubMed: 26799988]
13. “Darunavir, a New PI with Dual Mechanism: From a Novel Drug Design Concept to New Hope against Drug-Resistant HIV”Ghosh, AK., Chapsal, B., Mitsuya, H. Aspartic Acid Proteases as Therapeutic Targets. Wiley-VCH; Weinheim: 2010. p. 205-243.
14. Ghosh AK, Chapsal BD, Weber IT, Mitsuya H. Acc Chem Res. 2008; 41:78–86. [PubMed: 17722874]
15. “Design of the Anti-HIV Protease Inhibitor Darunavir”Ghosh, AK., Chapsal, BD. Introduction to Biological and Small-Molecule Drug Research and Development. Ganellin, CR.Roberts, SM., Jefferis, R., editors. Elsevier; Amsterdam: 2013. p. 355-384.
16. Ghosh AK, Dawson ZL, Mitsuya H. Bioorg Med Chem. 2007; 15:7576–7580. [PubMed: 17900913]
17. Koh Y, Nakata H, Maeda K, Ogata H, Bilcer G, Devasamudram T, Kincaid JF, Boross P, Wang YF, Tie Y, Volarath P, Gaddis L, Harrison RW, Weber IT, Ghosh AK, Mitsuya H. Antimicrob Agents Chemother. 2003; 47:3123–3129. [PubMed: 14506019]
18. Surleraux DLNG, Tahri A, Verschueren WG, Pille GME, de Kock HA, Jonckers THM, Peeters A, De Meyer S, Azijn H, Pauwels R, de Bethune MP, King NM, Prabu-Jeyabalan M, Schiffer CA, Wigerinck PBTP. J Med Chem. 2005; 48:1813–1822. [PubMed: 15771427]
19. On June 23, 2006, FDA approves Darunavir for HIV treatment-experienced patients, and on December 13, 2008 for treatment-naïve patients and pediatrics. Available at http://www.accessdata.fda.gov/scripts/cder/drugsatfda/index.cfm, (accessed September 2017).
20. Tie Y, Boross PI, Wang YF, Gaddis L, Hussian AK, Leshchenko S, Ghosh AK, Louis JM, Harrison RW, Weber IT. J Mol Biol. 2004; 338:341–352. [PubMed: 15066436]
21. Ghosh AK, Anderson DD, Weber IT, Mitsuya H. Angew Chem Int Ed. 2012; 51:1778–1802.Angew Chem. 2012; 124:1812–1838.
22. Yedidi RS, Maeda K, Fyvie WS, Steffey M, Davis DA, Palmer I, Aoki M, Kaufman JD, Stahl SJ, Garimella H, Das D, Wingfield PT, Ghosh AK, Mitsuya H. Antimicrob Agents Chemother. 2013; 57:4920–4927. [PubMed: 23877703]
23. Kovalevsky AY, Tie Y, Liu F, Boross PI, Wang YF, Leshchenko S, Ghosh AK, Harrison RW, Weber IT. J Med Chem. 2006; 49:1379–1387. [PubMed: 16480273]
24. Yedidi RS, Garimella H, Aoki M, Aoki-Ogata H, Desai DV, Chang SB, Davis DA, Fyvie WS, Kaufman JD, Smith DW, Das D, Wingfield PT, Maeda K, Ghosh AK, Mitsuya H. Antimicrob Agents Chemo-ther. 2014; 58:3679–3688.
25. Ghosh AK, Sridhar PR, Leshchenko S, Hussain AK, Li J, Kova-levsky AY, Walters DE, Wedekind JE, Grum-Tokars V, Das D, Koh Y, Maeda K, Gatanaga H, Weber IT, Mitsuya H. J Med Chem. 2006; 49:5252–5261. [PubMed: 16913714]

26. Ghosh AK, Sridhar PR, Kumaragurubaran N, Koh Y, Weber IT, Mitsuya H. ChemMedChem. 2006; 1:939–950. [PubMed: 16927344]
27. Couty F, David O, Larmanjat B, Marrot J. J Org Chem. 2007; 72:1058–1061. [PubMed: 17253837]
28. Fujii A, Hashiguchi S, Uematsu N, Ikariya T, Noyori R. J Am Chem Soc. 1996; 118:2521–2522.
29. Phillips AJ, Uto Y, Wipf P, Reno MJ, Williams DR. Org Lett. 2000; 2:1165–1168. [PubMed: 10804580]
30. Van Leusen AM, Hoogenboom BE, Siderius H. Tetrahedron Lett. 1972:2369–2372.
31. Pippel DJ, Mapes CM, Mani NS. J Org Chem. 2007; 72:5828–5831. [PubMed: 17585818]
32. Toth MV, Marshall GR. Int J Pept Protein Res. 1990; 36:544–550. [PubMed: 2090647]
33. Koh Y, Amano M, Towata T, Danish M, Leshchenko-Yashchuk S, Das D, Nakayama M, Tojo Y, Ghosh AK, Mitsuya H. J Virol. 2010; 84:11961–11969. [PubMed: 20810732]
34. Koh Y, Das D, Leschenko S, Nakata H, Ogata-Aoki H, Amano M, Nakayama M, Ghosh AK, Mitsuya H. Antimicrob Agents Chemother. 2009; 53:997–1006. [PubMed: 18955518]
35. Mahalingam B, Louis JM, Hung J, Harrison RW, Weber IT. Proteins Struct Funct Bioinf. 2001; 43:455–464.
36. Otwinowski, Z., Minor, W. Processing of X-ray Diffraction Data Collected in Oscillation Mode Methods in Enzymology, 276: Macromolecular Crystallography, Part A. Carter, CW., Jr, Sweet, RM., editors. Academic Press; New York: 1997. p. 307-326.
37. Shen CH, Wang YF, Kovalevsky AY, Harrison RW, Weber IT. FEBS J. 2010; 277:3699–3714. [PubMed: 20695887]
38. McCoy AJ, Grosse-Kunstleve RW, Adams PD, Winn MD, Storo-ni LC, Read RJ. J Appl Crystallogr. 2007; 40:658–674. [PubMed: 19461840]
39. Winn MD, Ballard CC, Cowtan KD, Dodson EJ, Emsley P, Evans PR, Keegan RM, Krissinel EB, Leslie AGW, McCoy A. Acta Crys-tallogr Sect D. 2011; 67:235–242.
40. Collaborative Computational Project Number 4. Acta Crystallogr Sect D. 1994; 50:760–763. [PubMed: 15299374]
41. Potterton E, Briggs P, Turkenburg M, Dodson E. Acta Crystallogr Sect D. 2003; 59:1131–1137. [PubMed: 12832755]
42. Sheldrick GM. Acta Crystallogr Sect A. 2008; 64:112–122. [PubMed: 18156677]
43. Sheldrick GM, Schneider TR. Methods Enzymol. 1997; 277:319–343. [PubMed: 18488315]
44. Emsley P, Lohkamp B, Scott WG, Cowtan K. Acta Crystallogr Sect D. 2010; 66:486–501. [PubMed: 20383002]
45. Emsley P, Cowtan K. Acta Crystallogr Sect D. 2004; 60:2126–2132. [PubMed: 15572765]
46. Schüttelkopf AW, van Aalten DMF. Acta Crystallogr Sect D. 2004; 60:1355–1363. [PubMed: 15272157]
47. Berman HM, Westbrook J, Feng Z, Gilliland G, Bhat TN, Weissig H, Shindyalov IN, Bourne PE. Nucleic Acids Res. 2000; 28:235–242. [PubMed: 10592235]

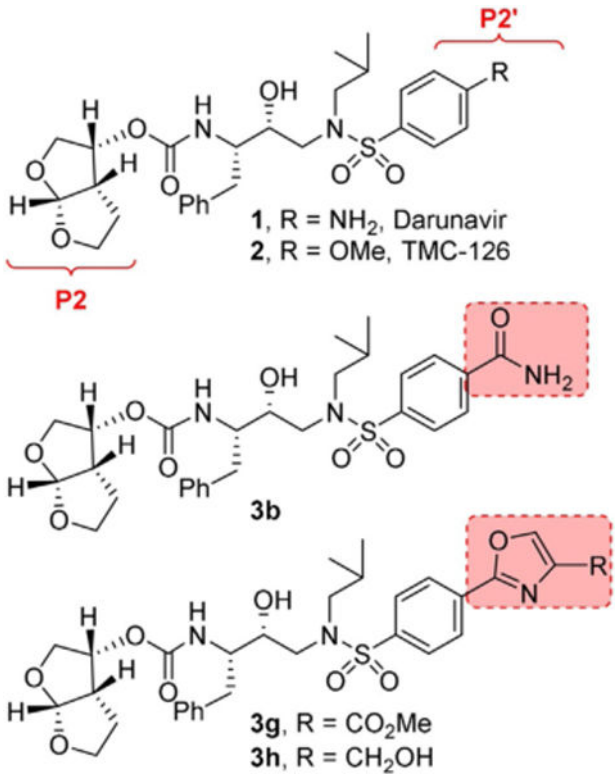

Figure 1.
Structures of HIV-1 protease inhibitors **1** and **2** and of novel inhibitors **3b**,**g**,**h**.

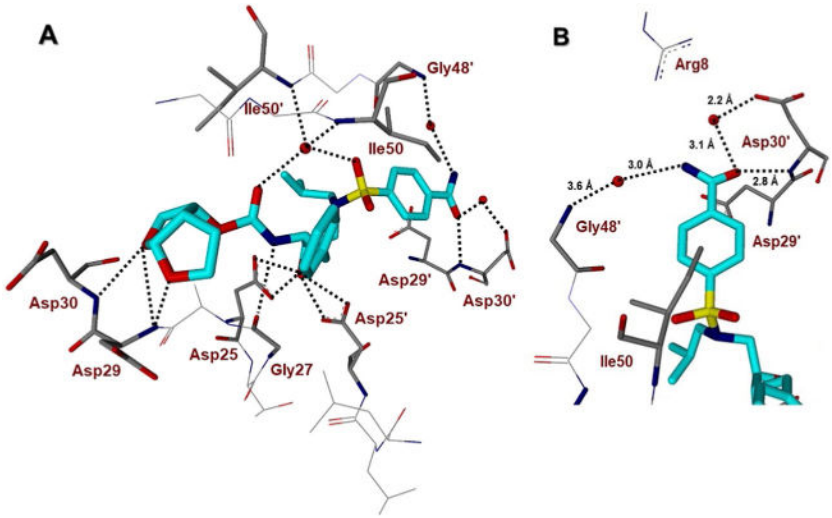

Figure 2.

A) Inhibitor **3b**-bound X-ray structure of HIV-1 protease. The major orientation of the inhibitor is shown. The inhibitor carbon atoms are shown in turquoise, water molecules are red spheres, and the hydrogen bonds are indicated by dotted lines. B) Specific hydrogen bonding interactions of carboxamide are shown. These interactions are indicated with respective distances.

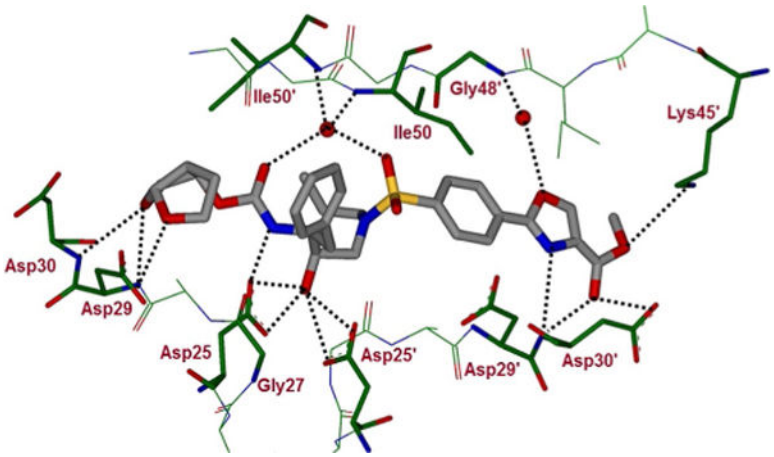

Figure 3.

Inhibitor **3g**-bound X-ray structure of HIV-1 protease. The major orientation of the inhibitor is shown. The inhibitor carbon atoms are shown in grey, water molecules are red spheres, and the hydrogen bonds are indicated by dotted lines (PDB ID: 6B4N).

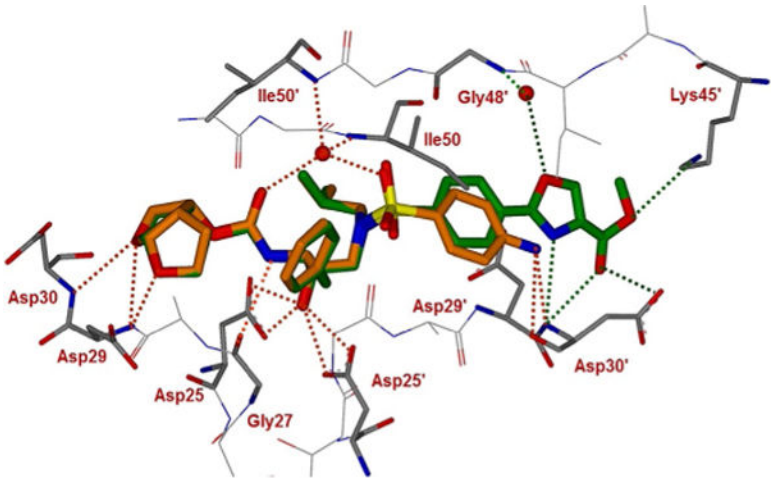

Figure 4.

An overlay of the X-ray crystal structure of DRV-bound HIV-1 protease (orange) with the X-ray structure of inhibitor **3g** (green)-bound HIV-1 protease.

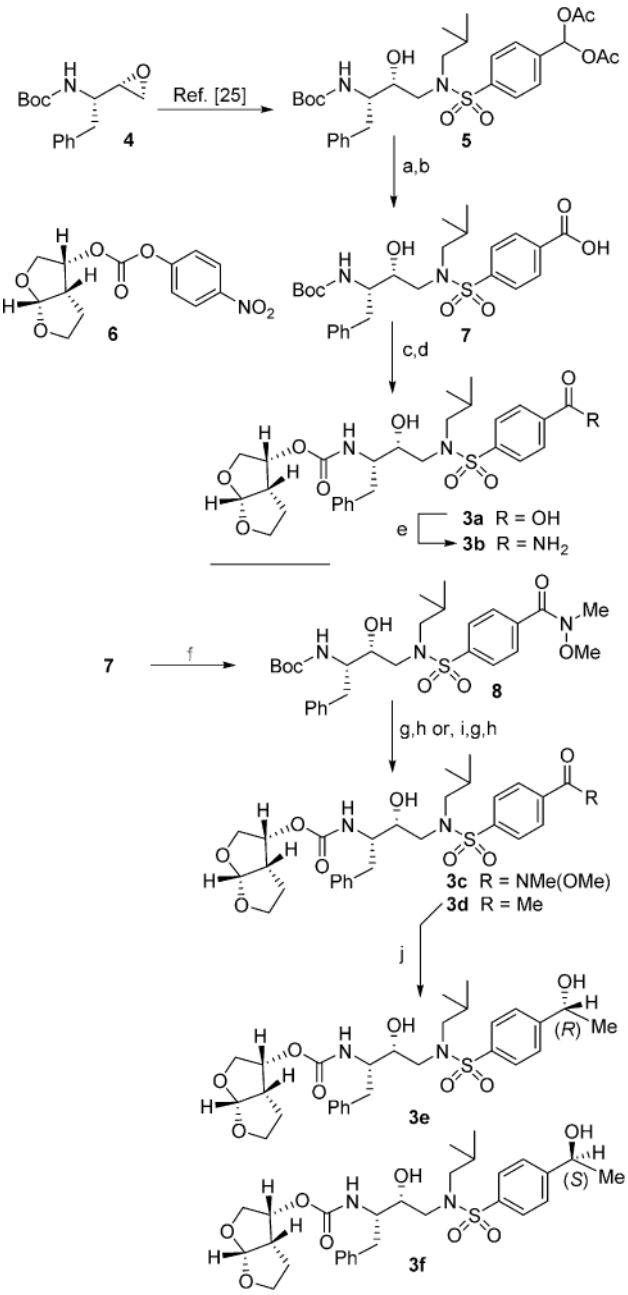

Scheme 1.

Reagents and conditions: a) K_2CO_3, MeOH, 23°C, 1 h, 98%; b) $NaClO_2$, *cis*-2-methyl-2-butene, NaH_2PO_4. H_2O, *t*BuOH-H_2O, 23°C, 50 min, 95%; c) TFA, CH_2Cl_2, 23°C, 3 h; d) **6**, *N*,*N*-DIPEA, MeCN/H_2O, 23°C, 3 days 89% (over two steps); e) pyridine, Boc_2O, $(NH_4)_2CO_3$, THF, 23 °C, 14 h, 76%; f) *i*BuOCOCl, NMM then MeNHOMe·HCl, dry CH_2Cl_2, −15°C →23°C, 12 h, 76%; g) TFA, CH_2Cl_2, 23 °C, 2 h; h) **6**, *N*,*N*-DIPEA, MeCN, 23°C, 5 days, 73–78%; i) MeMgBr (3 M in Et_2O), dry THF, −78°C, 4 h, 98%; j) RuCl[(R,R)-TsDPEN](mesitylene) for **3e** or RuCl(*p*-cymene)[(S,S)-Ts-DPEN] for 3f, TEA, HCOOH, dry CH_2Cl_2, 0°C →23°C, 7 h, 94–98 %.

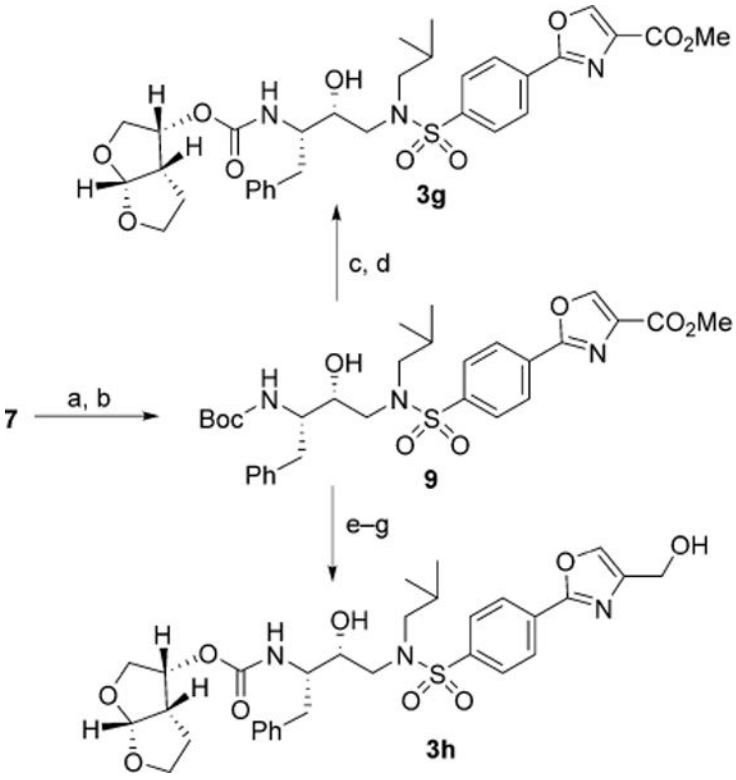

Scheme 2.

Reagents and conditions: a) D,L-Serine methyl ester hydrochloride, EDCI, HOBt, *N,N*-DIPEA, dry DMF, 0°C→23°C, 16 h, 91%; b) DAST, dry CH_2Cl_2, −78°C, 30 min, then $BrCCl_3$, DBU, dry CH_2Cl_2, 0°C→23°C, 2.5 h, 64% (over two steps); c) TFA, CH_2Cl_2, 23°C, 4 h; d) **6**, *N,N*-DIPEA, MeCN, 23°C, 6 days, 61% (over two steps); e) $NaBH_4$, EtOH, 0°C→23°C, 24 h, 65%; f) TFA, CH_2Cl_2, 23°C, 4 h; g) **6**, *N,N*-DIPEA, MeCN, 23°C, 5 days, 60% (over two steps).

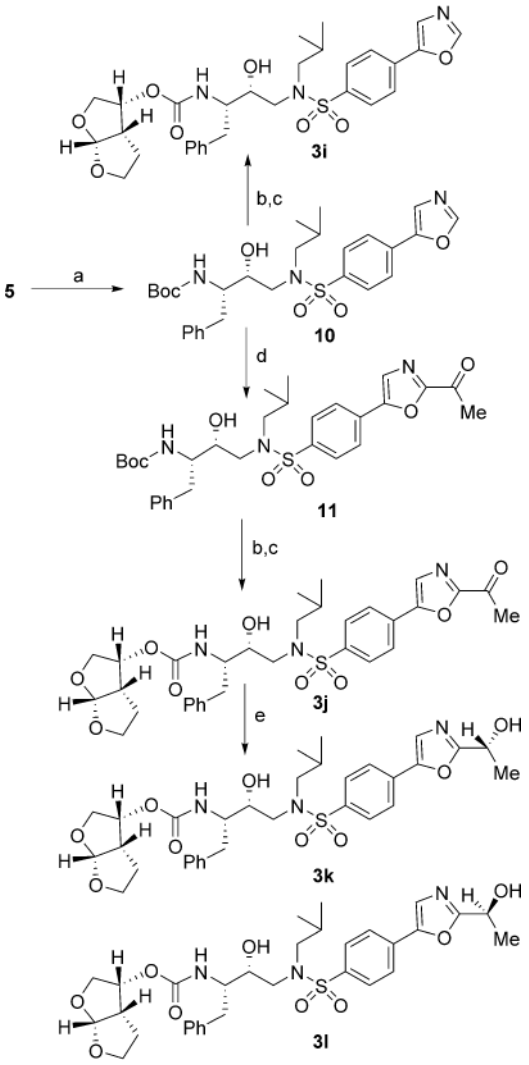

Scheme 3.

Reagents and conditions: a) TosMIC, K_2CO_3, MeOH, 55°C, 1.5 h, 96%; b) TFA, CH_2Cl_2, 23°C, 2.5 h; c) **6**, *N*,*N*-DIPEA, MeCN, 23°C, 4–7 days, 47–80% (over two steps); d) *i*PrMgCl, dry THF, 15°C, 40 min, then AcN(-Me)OMe, −15°C→23°C, 5 h, 79%; e) RuCl[(−*R*,*R*)-TsDPEN](mesitylene) for **3k** or RuCl(*p*-cymene)[(*S*,*S*)-Ts-DPEN] for **3l**, TEA, HCOOH, dry CH_2Cl_2, 0°C→23°C, 7 h, 95–97%.

Table 1

Structures and activity of inhibitors **3a**–**l**.

Entry	Inhibitor structure	K_i [pM][a]	IC_{50} [nM][b,c]
1.	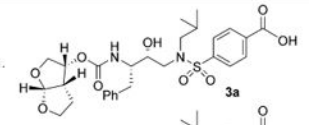 **3a**	12	>1000
2.	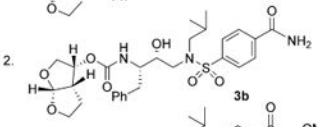 **3b**	8.9	45
3.	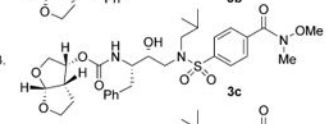 **3c**	192	130
4.	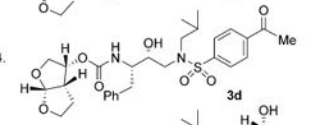 **3d**	9.7	2.0
5.	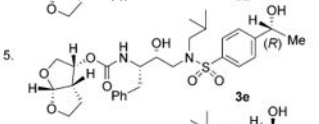 **3e**	9.9	4.0
6.	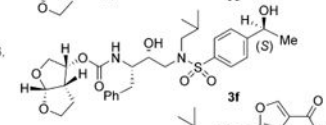 **3f**	46	nt
7.	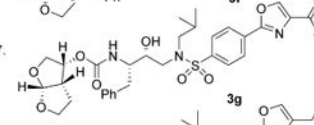 **3g**	27.9	6.2
8.	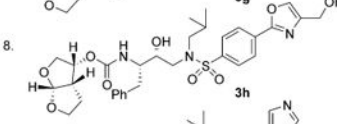 **3h**	49.7	3.9
9.	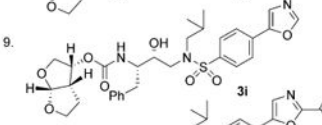 **3i**	126	2.8
10.	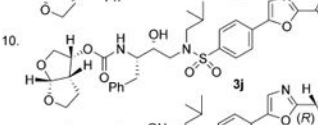 **3j**	119	2.8
11.	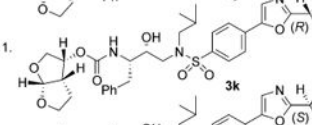 **3k**	37.3	3.2
12.	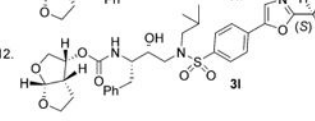 **3l**	21.7	nt

[a] K_i values represent at least five data points; the standard error in all cases was <7%. Darunavir exhibited K_i=16 pM.

[b] nt: Not tested.

[c] Values are the mean of at least three experiments; standard error in all cases was <5%. Darunavir exhibited IC_{50}=1.6 nM.

Table 2

Antiviral activity of two novel compounds against highly DRV-resistant HIV-1 variants.

HIV-1	IC_{50} [nM] (fold change)[a]		
	DRV	3g	3h
HIV-1_{NL4-3}	3.4	22	3.0
HIV-$1_{DRV^{R}P20}$	43 (13)	320 (15)	260 (88)
HIV-$1_{DRV^{R}P30}$	24 (71)	430 (20)	290 (99)
HIV-$1_{DRV^{R}P40}$	>1 (>297)	>1 (>46)	>1 (>337)

[a] MT-4 cells (1×10^{4}) were exposed to 50 $TCID_{50}$s of wild-type HIV-1_{NL4-3}, HIV-$1_{DRV^{R}P20}$, HIV-$1_{DRV^{R}P30}$, or HIV-$1_{DRV^{R}P40}$ and cultured in the presence of various concentrations of each PI, and the IC_{50} values were determined using the p24 assay. The amino acid substitutions identified in protease of HIV-$1_{DRV^{R}P20}$, HIV-$1_{DRV^{R}P30}$, and HIV-$1_{DRV^{R}P40}$ HIV-1_{NL4-3} include L10I/I15V/K20R/L24I/V32I/M36I/M46L/L63P/V82A/L89M, L10I/I15V/K20R/L24I/V32I/M36I/M46L/L63P/K70R/V82A/I84V/L89M, and L10I/I15V/K20R/L24I/V32I/L33F/M36I/M46L/I54M/L63P/K70Q/V82I/I84V/L89M, respectively. All assays were conducted in triplicate, and the data are mean values derived from the results of three independent experiments; standard error in all cases <5%.